

## Effect of cross-beam on stresses revealed in orthotropic steel bridges

Abdullah Fettahoglu \*

*Department of Civil Engineering, Yildiz Technical University, Esenler 34220, Istanbul, Turkey*

*(Received February 10, 2013, Revised May 12, 2014, Accepted May 14, 2014)*

**Abstract.** Orthotropic steel highway bridges exist almost everywhere in world, especially in Europe. The design of these bridges started very early in 20th century and ended with a conventional orthotropic steel bridge structure, which is today specified in DIN FB 103. These bridges were mostly built in 1960's and exhibit damages in steel structural parts. The primary reason of these damages is the high pressure that is induced by wheel- loads and therefore damages develop especially in heavy traffic lanes. Constructive rules are supplied by standards to avoid damages in orthotropic steel structural parts. These rules are first given in detail in the standard DIN 18809 (Steel highway- and pedestrian bridges- design, construction, fabrication) and then in DIN- FB 103 (Steel bridges). Bridges built in the past are today subject to heavier wheel loads and the frequency of loading is also increased. Because the vehicles produced today in 21st century are heavier than before and more people have vehicle in comparison with 20th century. Therefore dimensioning or strengthening of orthotropic steel bridges by using stiffer dimensions and shorter spans is an essence. In the scope of this study the complex geometry of conventional steel orthotropic bridge is generated by FE-Program and the effects of cross beam web thickness and cross beam span on steel bridge are assessed by means of a parameter study. Consequently, dimensional and constructional recommendations in association with cross beam thickness and span will be given by this study.

**Keywords:** finite elements; orthotropic steel bridges; cross-beams

---

### 1. Introduction

In Germany there are a lot of orthotropic bridges, which shall be repaired and reinforced because of damages developed in steel structural parts. Most of these bridges were built in 1960s after World War II. Since then the weight of vehicles passing over these bridges, the traffic intensity and the frequency of passing of vehicles (loading frequency) have increased. As a result these bridges are loaded under loads which are much more than their design loads. The causes of damages developed in bridges are divided briefly into two main groups: qualitative and quantitative causes. Qualitative causes of damages are false workmanship, bad design of bridge (false engineering), and using inadequate or non-qualitative material. Quantitative causes are thin deck plate, thin or less longitudinal ribs, thin crossbeams or long span of cross beams. In this research the cross section of bridge is chosen as per DIN FB 103 (Deutsches Institut für Normung

---

\*Corresponding author, Ph.D. Student, E-mail: [abdullahfettahoglu@gmail.com](mailto:abdullahfettahoglu@gmail.com)



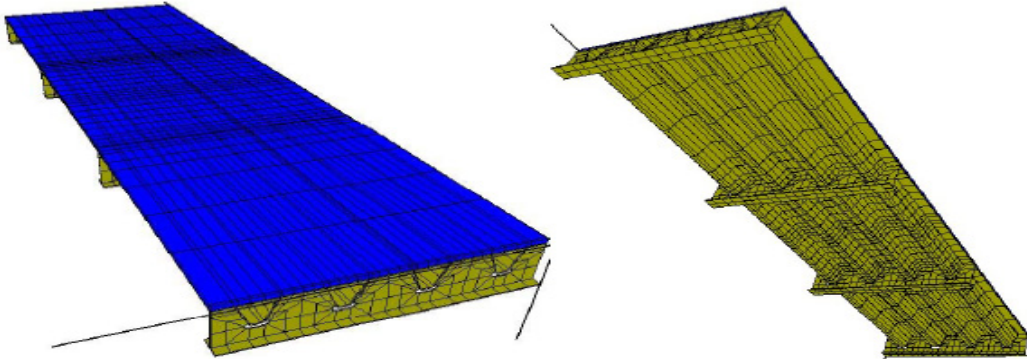


Fig. 3 Huurman's *et al.* (2002) FE- model to analyze orthotropic steel bridges

are chosen as short as possible. As a result the bridge spans 6 m and has stiffened main girders at supports, normal main girders at field (outside support areas), 2 exterior- 5 interior ribs, 1 rib on main girder and 1 rib in pedestrian road. To decrease further the number of nodal unknowns solely the quarter of the bridge shown in Figs. 6(a) and (b) is modeled by means of FE- program (ANSYS 2010) using SHELL 181 shell element formulation. Both geometric and material nonlinearity of this element are taken into account in this study. The material nonlinearity of steel is incorporated into FE- simulations using Bilinear-Kinematic-Hardening law, which conforms to prEN 1993-1-5: 2004(E) Table C2.c. and given in Fig. 4. This theory comprises yield function, hardening and flow rules. Here, only general nonlinearity equations are given, more details about geometric and material nonlinearity can be found in (Mendelson 1968), (Cook *et al.* 1989) and (Simo and Taylor 1985).

The general equation of nodal unknowns are given as

$$[K] \cdot \{u\} = \{F^a\} \quad (1)$$

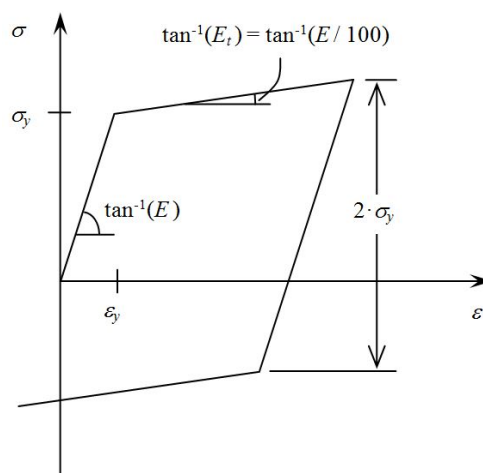


Fig. 4 Stress strain relationship of steel

whereas

$$\begin{aligned} [K] &= \text{Stiffness matrix,} \\ \{u\} &= \text{Displacements (nodal unknowns) vector,} \\ \{F^a\} &= \text{Load vector} \end{aligned}$$

If  $[K]$  is a function of  $\{u\}$ , Eq. (1) becomes a nonlinear equation. The Newton- Raphson-Method makes the iterative solution of nonlinear equation system possible and given as, (Cook *et al.* 1989)

$$[K_i^T] \cdot \{\Delta u_i\} = \{F^a\} - \{F_i^{nr}\} \quad (2)$$

$$\{u_{i+1}\} = \{u_i\} + \{\Delta u_i\} \quad (3)$$

whereas

$$\begin{aligned} [K_i^T] &= \text{Tangential stiffness matrix,} \\ i &= \text{Number of current iteration,} \\ [F_i^{nr}] &= \text{Vector of internal element forces derived from stresses.} \end{aligned}$$

$[K_i^T]$  and  $[F_i^{nr}]$  are functions of  $\{u_i\}$ . The right side of Eq. (2) is residual-load vector. This vector is the measure of loads, which remains out of equilibrium.

Material nonlinearity theory comprises yield function, hardening and flow rules.

The yield criterion proposes a stress state, after which material starts to yield. This criterion is a yield function of stress tensor and equals to equivalent (von Mises) stress with Kinematic Hardening

$$\sigma_e = \left[ \frac{3}{2} (\{s\} - \{\alpha\})^T [M] (\{s\} - \{\alpha\}) \right]^{1/2} \quad (4)$$

whereas

$$\begin{aligned} \{s\} &= \text{deviatoric stress vector} = \{\sigma\} - \sigma_m [111000]^T \\ \{\alpha\} &= \text{Backstress or displacement vector of yield surface.} \end{aligned} \quad (5)$$

$$\{\alpha\} = C \int d\{\varepsilon^{pl}\} = [\{\alpha_\sigma\} \{\alpha_\tau\}]^T \quad (6)$$

$$\{\sigma\} = \text{Stress vector} = [\sigma_x \ \sigma_y \ \sigma_z \ \tau_{xy} \ \tau_{yz} \ \tau_{xz}]^T \quad (7)$$

$$\sigma_m = \text{Hydrostatic stress} = \frac{1}{3} (\sigma_x + \sigma_y + \sigma_z) \quad (8)$$

$$C = \frac{2}{3} \frac{E \cdot E_T}{E - E_T} \quad (9)$$

As per von Mises-yield criterion yielding does not depend on hydrostatic stress. When the equivalent stress becomes equal to the uniaxial yield stress ( $\sigma_y$ ), the material starts to yield. As a result yield criterion is given as

$$F = \left[ \frac{3}{2} (\{s\} - \{\alpha\})^T [M] (\{s\} - \{\alpha\}) \right]^{1/2} - \sigma_y = 0 \quad (10)$$

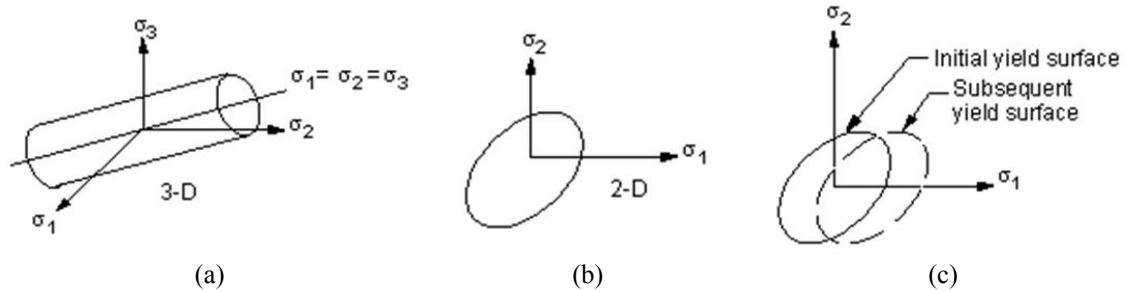


Fig. 5 (a) 3D- Yield surface; (b) 2D- Yield surface; and (c) 2D moving of yield surface (hardening)

Table 1 Material properties

Yield stress of steel ( $f_y$ )	355 N/mm <sup>2</sup>	Shear module ( $G$ )	81000 N/mm <sup>2</sup>
Ultimate strength ( $f_u$ )	510 N/mm <sup>2</sup>	Poisson ratio ( $\nu$ )	0.3
Elasticity module ( $E$ )	210000 N/mm <sup>2</sup>	Density ( $\rho_{steel}$ )	78.5 kN/m <sup>3</sup>

Fig. 5 illustrates yield surface in 2D and 3D spaces and its moving as per applied stress values (hardening).

The direction and amplitude of plastic strain are determined using Eq. (11)

$$\{d\epsilon^{pl}\} = \lambda \left\{ \frac{\partial Q}{\partial \sigma} \right\} \quad (11)$$

whereas

$\lambda$  = Plastic constants, which sets the value of plastic strain.

$Q$  = Plastic potential function, which sets the direction of plastic strain.

Here  $Q$  is equal to yield function given in Eq. (10) and plastic strain develops perpendicular to yield surface. Therefore this flow rule is called as Associative Flow Rule. The selected steel material is S 355. In accordance with Capital II of DIN FB 103 the yield stress and strength values are given in Table 1.

The loading on the bridge is given in Fig. 6(a)). Here symmetry conditions according to midpoint of bridge are used to reduce the number of nodal unknowns. The maximum von Mises stress and displacement under this loading amounts 255.279 MPa and 1.729 mm respectively. The deformed shape of bridge is 150 times scaled up for a better illustration of the results and given in Fig. 6(b)).

### 3. Effect of cross – Beam span on stresses revealed in steel bridge

This chapter presents the results of the parameter study of cross-beam span, which emerges the effect of this span on the stress and displacements developed in steel structural parts. All dimensions of the bridge (except cross-beam span) defined in FE- model are kept constant, while cross-beam span increases. Cross-beam spans of simulations QABST2000, BB, QABST4000 and

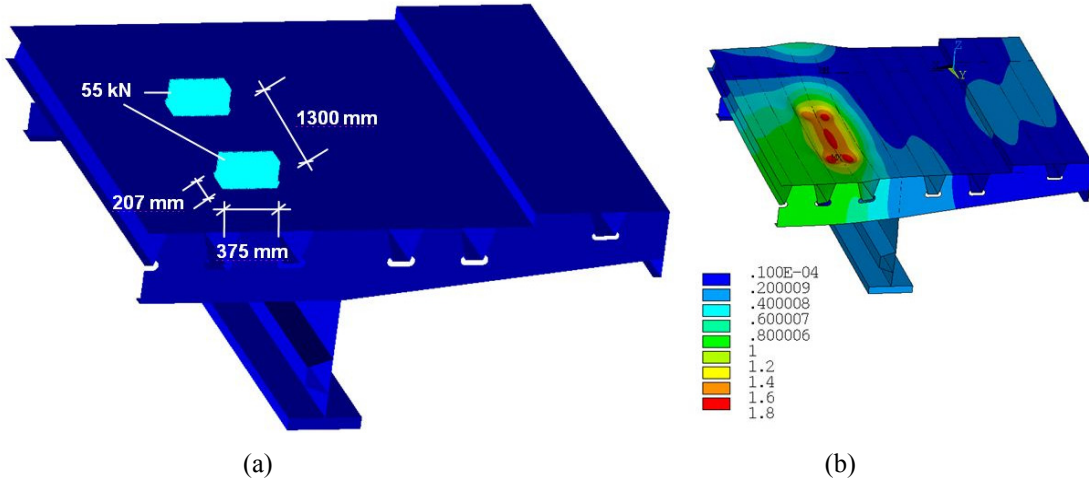


Fig. 6 (a) Wheel loads on quarter of bridge; (b) displacement vector under wheel loads, when cross-beam span and web thickness are 3 m and 14 mm respectively

QABST5000 are 2, 3, 4 and 5 m respectively. The results of simulations are given in figures, in which max. von Mises stress and displacement values on load bearing steel parts are presented. In figures deformed shape is given at the left side, whereas von Mises stress values are given at the right side. In the left figure vertical deformations are given based on nodal (averaged) values. Here MX means max. vertical displacement, whereas MN means min. vertical displacement. The symbol UZ designates the point where max. von Mises stress occurs. For instance in the left figure the value of UZ designates the point of max. von Mises stress. In the right figure max. von Mises stress value is given based on element results (non averaged value). Briefly, the place and elevation of max. von Mises stress is pictured in the left figure and the value of this von Mises

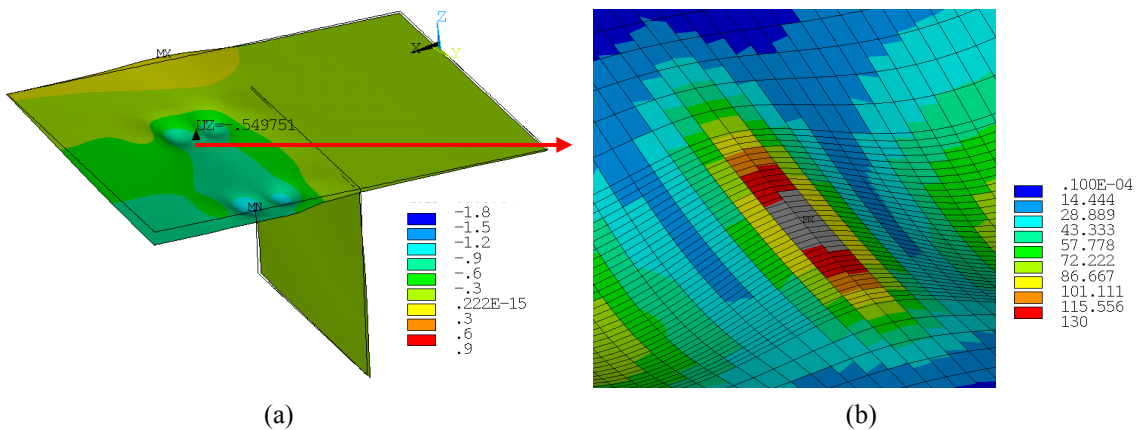


Fig. 7 Cross-beam span is 2 m: (a) vertical displacements of deck plate and main girder. Max. displacement = + 0.308787 mm. Min. displacement = - 1.135 mm; (b) max. von Mises-stress = 136.602 MPa

stress is given in the right figure. Max. values of von Mises stresses are the indicators of potential damages, so that these values are used in the assessment of results. The wheel loads are located direct on one web of interior rib, which exists next to main girder. On the other web of interior rib there is no load. This loading condition leads bending and twisting of this rib, which is welded to cross-beam at lateral sides, to deck plate at top and goes through cut- out of cross-beam at the bottom. The max. von Mises stress rises at this cut- out of cross-beam. Results of these FE-analysis are given below in Figs. 7 to 18.

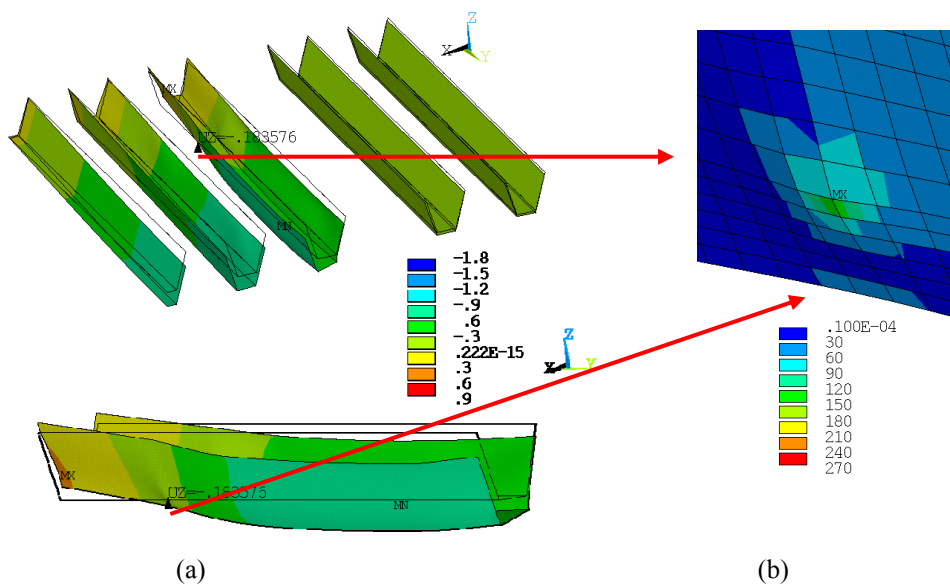


Fig. 8 Cross-beam span is 2 m: (a) vertical displacements of ribs. Max. displacement = + 0.352126 mm. Min. displacement = - 0.81561 mm; (b) max. von Mises-stress = 150.785 MPa

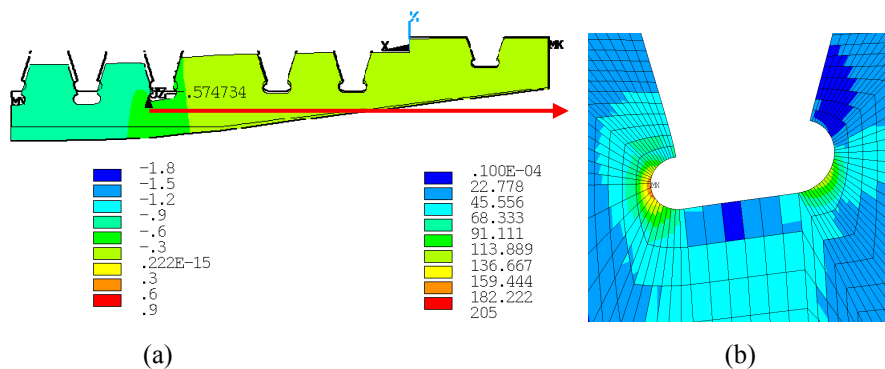


Fig. 9 Cross-beam span is 2 m: (a) vertical displacements of cross-beam. Max. displacement = - 0.031811 mm. Min. displacement = - 0.697488 mm; (b) max. von Mises-stress = 186.149 MPa

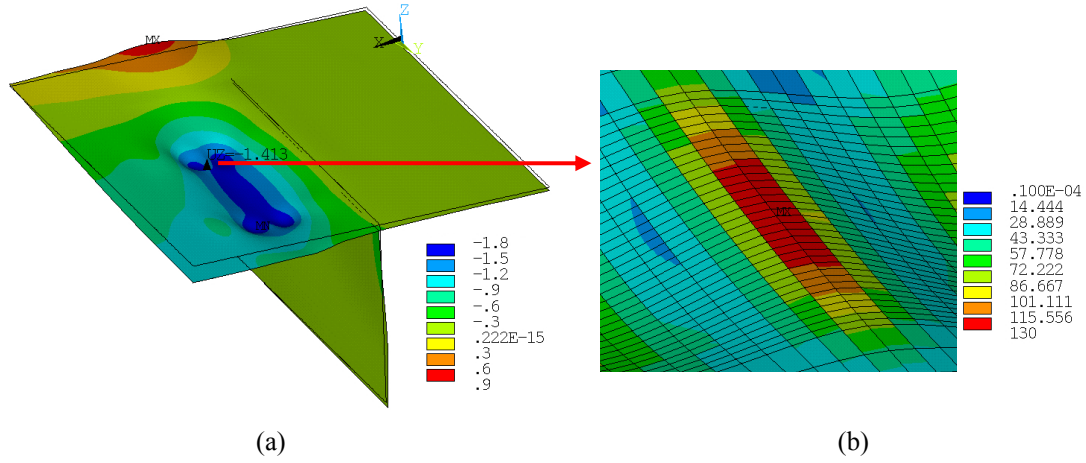


Fig. 10 Cross-beam span is 3 m: (a) vertical displacements of deck plate and main girder. Max. displacement = + 0.77646 mm. Min. displacement = - 1.729 mm; (b) max. von Mises-stress = 126.652 MPa

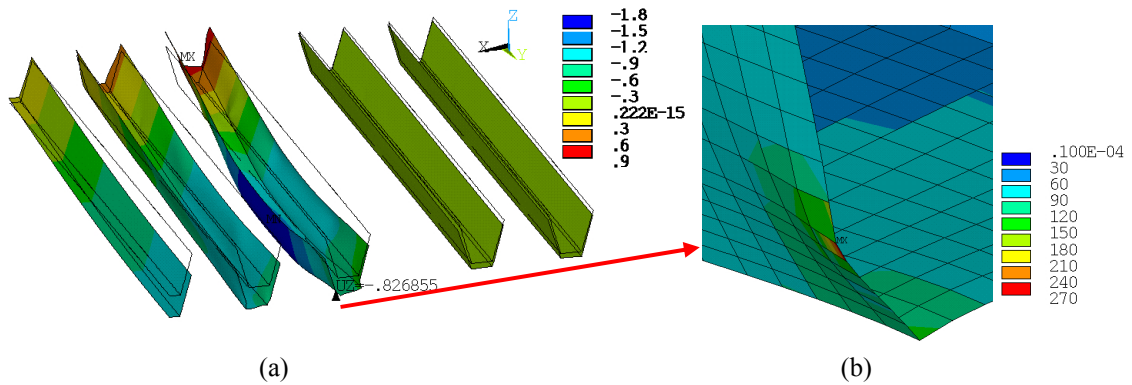


Fig. 11 Cross-beam span is 3 m: (a) vertical displacements of ribs. Max. displacement = + 0.787684 mm. Min. displacement = - 1.67 mm; (b) max. von Mises-stress = 255.279 MPa

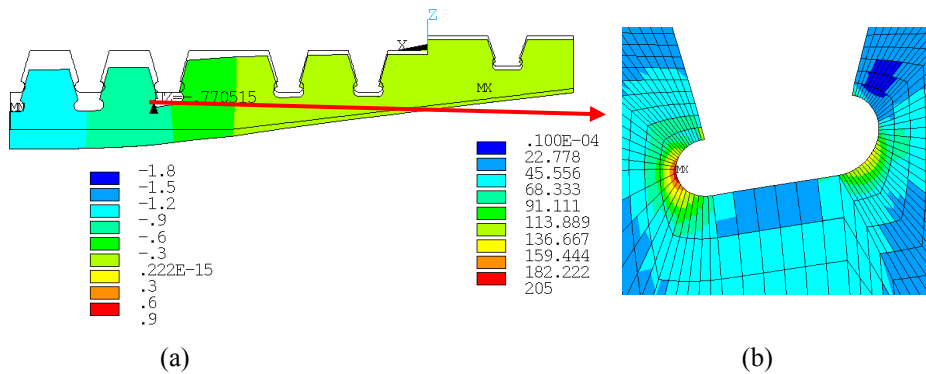


Fig. 12 Cross-beam span is 3 m: (a) vertical displacements of cross-beam. Max. displacement = - 0.159623 mm. Min. displacement = - 0.945902 mm; (b) max. von Mises-stress = 201.549 MPa

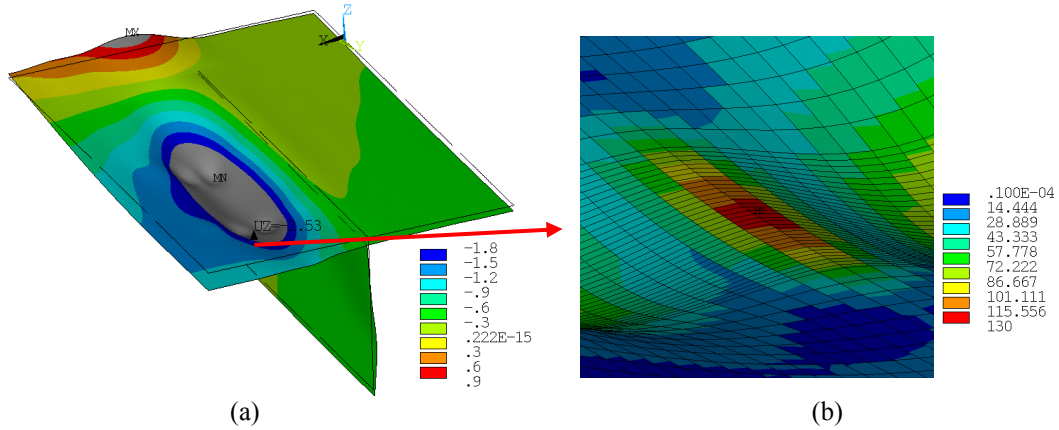


Fig. 13 Cross-beam span is 4 m: (a) vertical displacements of deck plate and main girder. Max. displacement = + 1.169 mm. Min. displacement = - 2.939 mm. These values exceed the contour limits (- 1.8 mm and + 0.9 mm) and displayed with gray colour; (b) max. von Mises-stress = 119.256 MPa

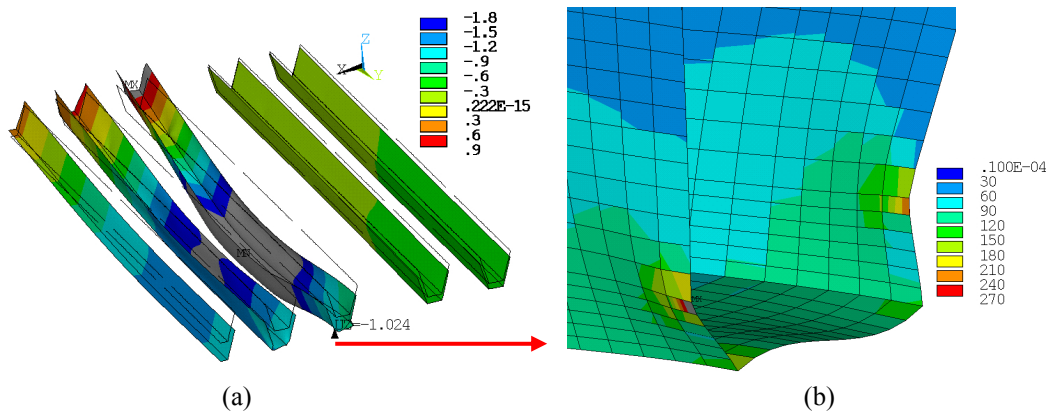


Fig. 14 Cross-beam span is 4 m: (a) vertical displacements of ribs. Max. displacement = +1.128 mm. Min. displacement = - 2.855 mm. These values exceed the contour limits (- 1.8 mm and + 0.9 mm) and displayed with gray colour; (b) max. von Mises-stress = 341.398 MPa

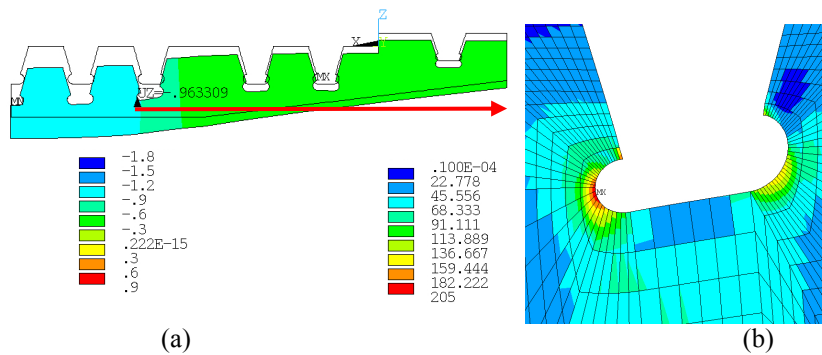


Fig. 15 Cross-beam span is 4 m: (a) vertical displacements of cross-beam. Max. displacement = - 0.331533 mm. Min. displacement = - 1.179 mm; (b) max. von Mises-stress = 204.471 MPa

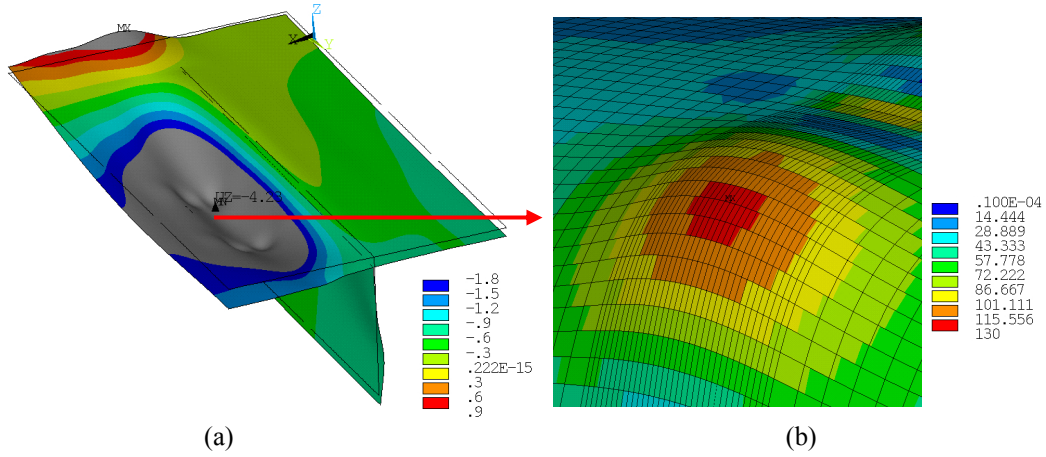


Fig. 16 Cross-beam span is 5 m: (a) vertical displacements of deck plate and main girder. Max. displacement = + 1.422 mm. Min. displacement = - 4.293 mm. These values exceed the contour limits (- 1.8 mm and + 0.9 mm) and displayed with gray colour; (b) max. von Mises-stress = 119.182 MPa

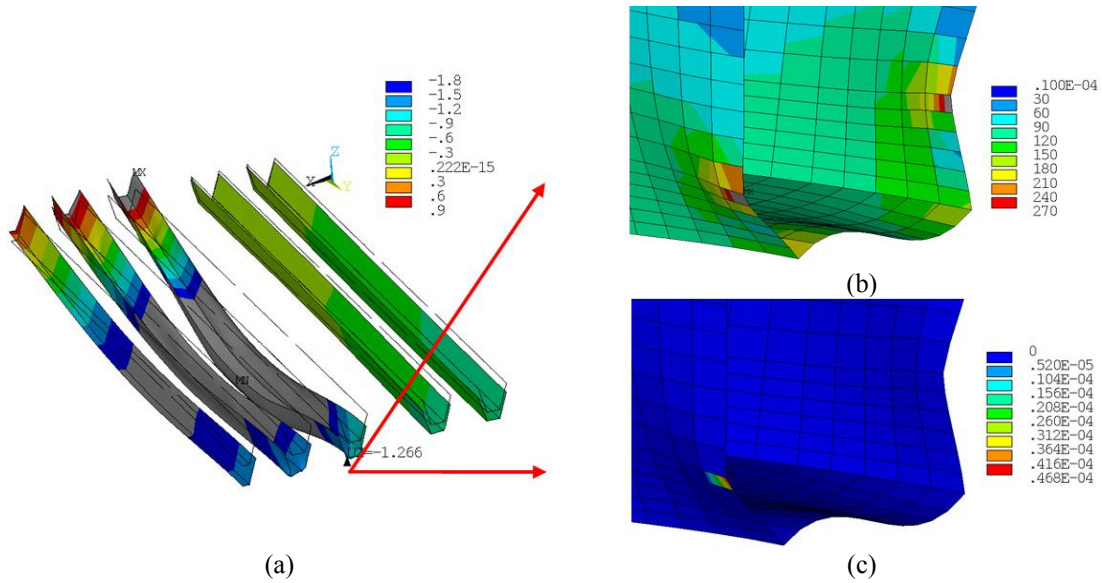


Fig. 17 Cross-beam span is 5 m: (a) vertical displacements of ribs. Max. displacement = + 1.367 mm. Min. displacement = - 4.197 mm. These values exceed the contour limits (- 1.8 mm and + 0.9 mm) and displayed with gray colour; (b) max. von Mises-stress = 355.099 MPa; and (c) distribution of plastic strain

#### 4. Effect of cross – Beam web thickness on stresses revealed in steel bridge

This chapter investigates the change in stresses of steel structural parts, if cross-beam web thickness changes. For that reason, all other dimensions of the bridge defined in FE- model keep constant, while cross-beam web thickness increases from 14 mm to 16, 18 and 20 mm respectively.

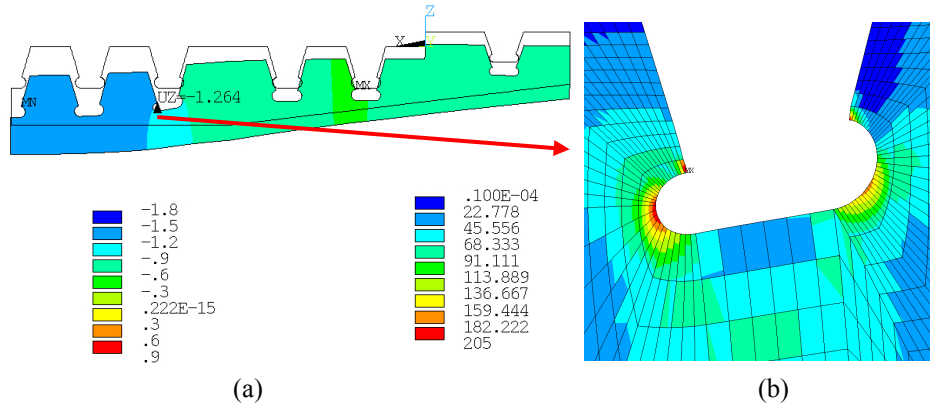


Fig. 18 Cross-beam span is 5 m: (a) vertical displacements of cross-beam. Max. displacement =  $-0.579947$  mm. Min. displacement =  $-1.448$  mm; (b) max. von Mises-stress =  $213.529$  MPa

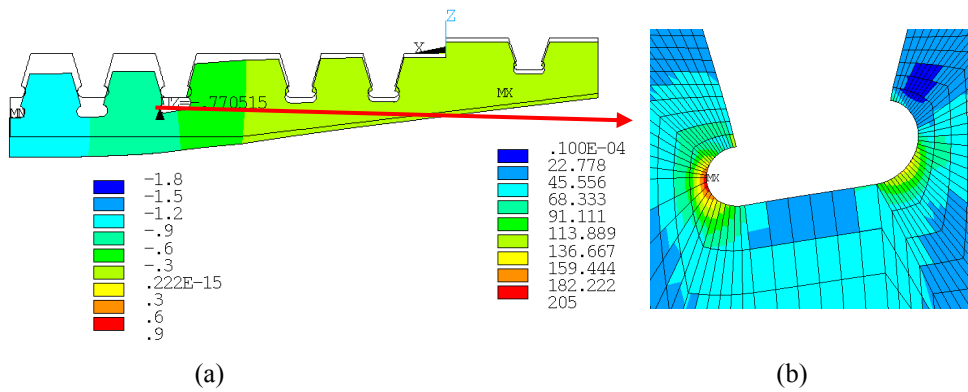


Fig. 19 Cross-beam web thickness is 14 mm: (a) vertical displacements of cross-beam. Max. displacement =  $-0.159623$  mm. Min. displacement =  $-0.945902$  mm; (b) max. von Mises-stress =  $201.549$  MPa

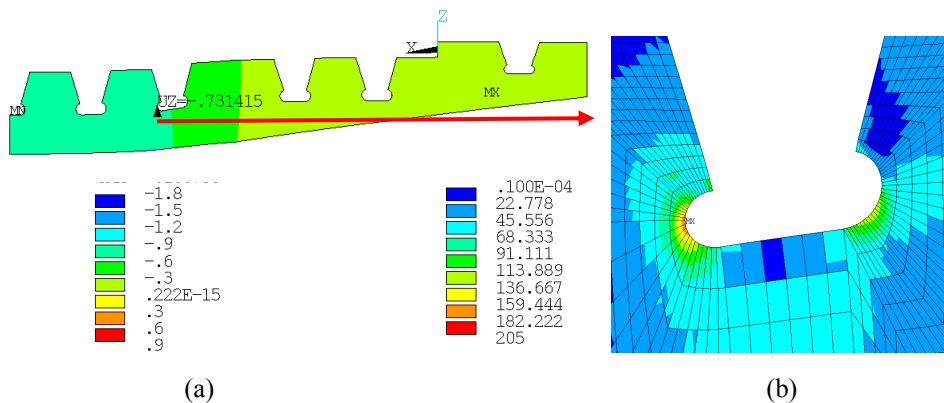


Fig. 20 Cross-beam web thickness is 16 mm: (a) vertical displacements of cross-beam. Max. displacement =  $-160758$  mm. Min. displacement =  $-0.89795$  mm; (b) max. von Mises-stress =  $180.448$  MPa

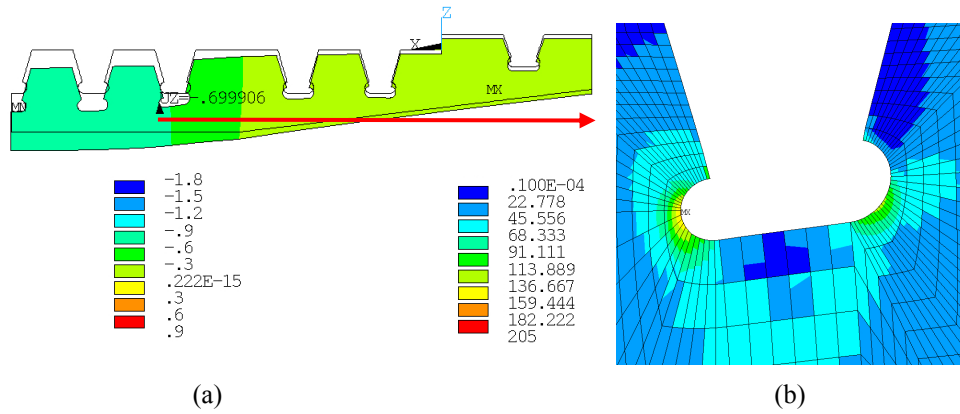


Fig. 21 Cross-beam web thickness is 18 mm: (a) vertical displacements of cross-beam. Max. displacement =  $-0.162599$  mm. Min. displacement =  $-0.858806$  mm; (b) max. von Mises-stress =  $163.540$  MPa

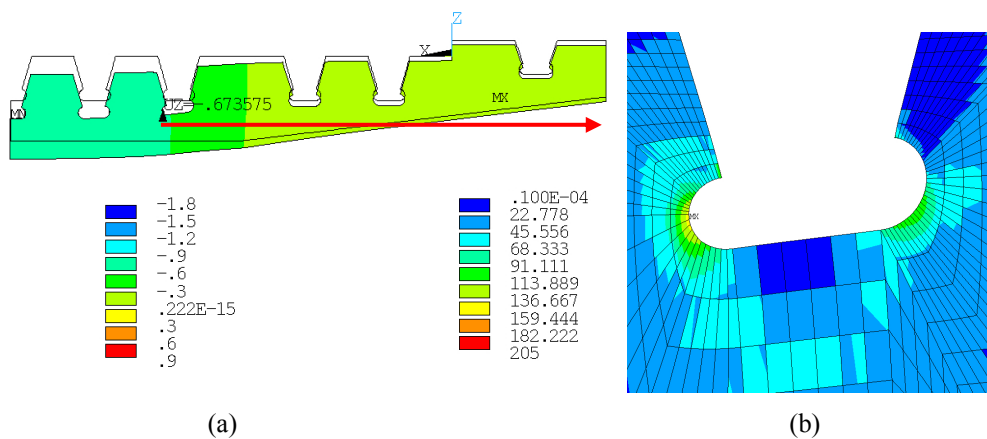


Fig. 22 Cross-beam web thickness is 20 mm: (a) vertical displacements of cross-beam. Max. displacement =  $-0.164775$  mm. Min. displacement =  $-0.825762$  mm; (b) max. von Mises-stress =  $149.661$  MPa

Here the cross-beam span is always taken as 3 m in all simulations. Results show that any change in cross-beam web thickness has almost no effect on deck plate and rib stresses. The change of stresses in cross-beam itself are given in Figs. 19 to 22.

## 5. Discussions

While cross-beam span increases, the deflections of deck plate, especially direct under wheel loads, increases heavily, nevertheless they still remain in elastic range. Max. von Mises-Stress emerges at the top face of deck plate, when cross-beam span is 2, 3 and 4 m. At cross-beam span of 5 m, max. von Mises-Stress emerges at the bottom face of deck plate direct under wheel loads. Stresses in deck plate decrease inverse proportional to cross-beam span, until it takes the value of 5 m. Apparently, the stresses in deck plate will increase proportional to cross-beam span after 5 m

span value, since the sign of bending moment under wheel loading changes. at 5 m span of cross-beam. As a result local effects (stresses & deflections) will be higher at cross-beam span of 6 m than cross-beam span of 5 m. With respect to stresses and deflections emerge in ribs, cross-beam span is of great importance, since the max. value of von Mises-Stress (indicator of damage) takes values from 150.785 MPa to 355.099 MPa, while cross-beam span rises from 2 to 5 m. As cross-beam span increases, twisting of the rib, which is under wheel load, becomes larger and

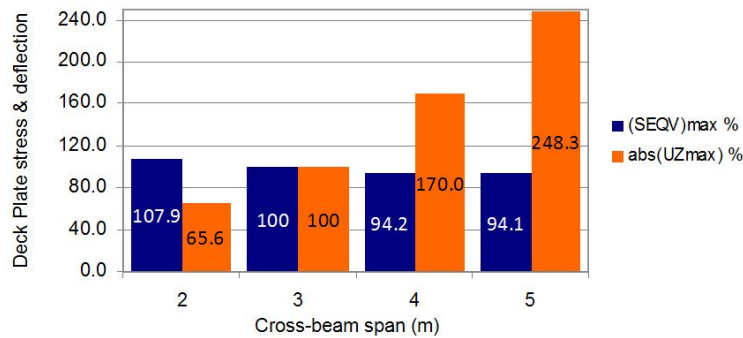


Fig. 23 Variation of max. von Mises-Stress & deflection in deck plate depending on cross-beam span

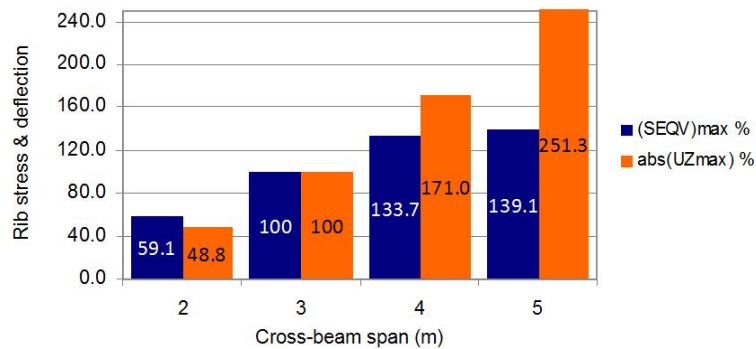


Fig. 24 Variation of max. von Mises-Stress & deflection in ribs depending on cross-beam span

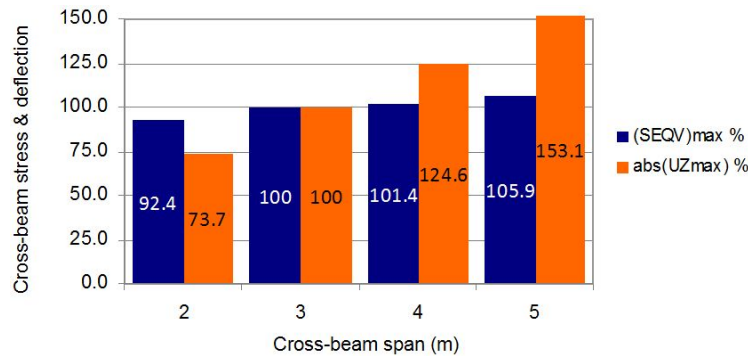


Fig. 25 Variation of max. von Mises-Stress & deflection in cross-beam depending on cross-beam span

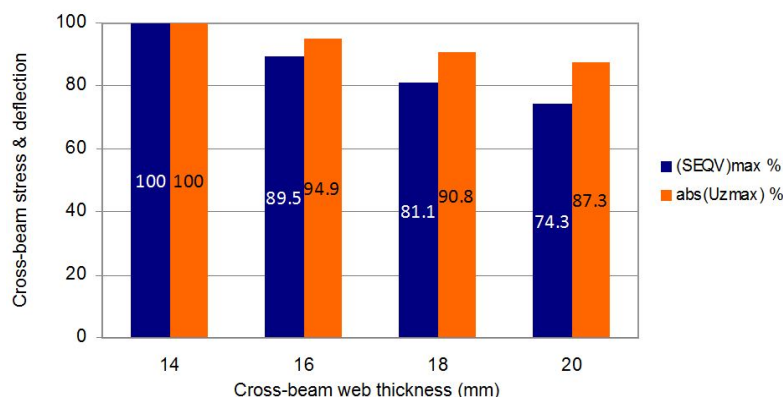


Fig. 26 Variation of max. von Mises-Stress & deflection in cross-beam depending on cross-beam web thickness

results in higher stresses at rib to cross-beam connection. For instance at the cross-beam span of 2 m, twisting of the rib is very small, so that the bending is dominant on the deformed shape of the rib. This result can be obviously seen from the comparison of Figs. 8 and 17. Regarding cross-beam itself, increasing its span yields in increase of dead load on cross-beam and the moment arm of wheel loads. These effects cause slight increases of stresses and deflections in cross-beam itself.

Because of increasing cross-beam web thickness, there exist almost no change in stresses and deflections develop in deck plate and ribs. The increase and so strengthening cross-beam web causes decreasing of shear force and so decreasing of tooth stresses in cross-beam web. The amount of this decrease in stress and deflection values is illustrated in Fig. 26 below.

## 6. Conclusions

It is seen from the results that the increase of cross-beam span from 2 m to 5 m causes very slight decrease of deck plate stresses, but heavily increase of deck plate deflections. With regard to steel load bearing parts of bridge all these stresses and deflections stay in elastic limits and have no hazard on the bridge. Nevertheless, the excessive deflections of deck plate can result in irreversible vertical displacements in asphalt wearing courses lying on deck plate and as a result rut formations can occur in asphalt. In terms of longitudinal ribs, stresses and deflections are highly affected by cross-beam span. At 5 m of cross-beam span rib material starts to yield. A cross-beam span between 3 and 4 m is recommended for the bridge analyzed in this study. Too small cross-beam spans like between 2 and 3 m are found to be very conservative under wheel loads. Regarding cross-beam itself, the increase of its span leads to slight increase of stresses and deflections in cross-beam. Therefore it is concluded that the stresses in cross-beam are allowed not to be considered, when determining cross-beam span of the bridge. As for cross-beam web thickness, it has no effect on the stresses develop in deck plate and ribs, but has effect on the stresses develop in cross-beam itself, as expected.

## References

- ANSYS (2010), User Manuals: Swanson Analysis System, USA.
- Cook, D.R., Malkus, D.S. and Plesha, M.E. (1989), *Concepts and Applications of Finite Element Analysis*, John Wiley & Sons, New York, NY, USA.
- Deutsches Institut für Normung Fachbericht (DIN FB) 103 (2003), Steel bridges, Berlin, Germany.
- Deutsches Institut für Normung Fachbericht (DIN) 18809 (1987), Steel road bridges and foot bridges; design and construction, Berlin, Germany.
- Fettahoğlu, A. (2012), "Effect of deck plate thickness on the structural behaviour of steel orthotropic highway bridges", *Adv. Civil Eng.*, Ankara, Turkey, October.
- Fettahoğlu, A. and Bekiroğlu, S. (2012), "Effect of kinematic hardening in stress calculations", *Adv. Civil Eng.*, Ankara, Turkey, October.
- Günther, G.H., Bild, St. and Sedlacek, G. (1985), "Zur Frage der Haltbarkeit von Fahrbahnbelägen auf stählernen Straßenbrücken", *Der Stahlbau*, **11**, 336-342.
- Huurman, Name of authors (2002), "3D-FEM for the estimation of the behaviour of asphaltic surfacings on orthotropic steel deck bridges", *Proceedings of the 3<sup>rd</sup> International Symposium on 3D Finite Element for Pavement Analysis, Design & Research*, Amsterdam, The Netherlands, April.
- Jong, de F.B.P. (2007), "Renovation techniques for fatigue cracked orthotropic steel bridge decks", Dissertation, Delft University of Technology, Faculty of Civil Engineering and Geosciences.
- Kozy, B., Connor, R., Paterson, D. and Mertz, D. (2011), "Proposed revisions to the AASHTO LRFD bridge design specifications for orthotropic steel deck bridges", *J. Bridge Eng.*, **16**(6), 759-767.
- Medani, T.O. (2006), "Design principles of surfacing on orthotropic steel bridge decks", Dissertation, Delft University of Technology, Faculty of Civil Engineering and Geosciences, The Netherlands.
- Mendelson, A. (1968), *Plasticity: Theory and Application*, The Macmillan Company, New York, NY, USA.
- Miki, C. (2006), "Fatigue damage in orthotropic steel bridge decks and retrofit works", *Int. J. Steel Struct.*, **6**(4), 255-267.
- prEN 1993-1-5 (2004), Design of Steel Structures, Plated Structural Elements, Brussels, Belgium.
- Sim, H.B., Uang, C.M. and Sikorsky, C. (2009), "Effects of fabrication procedures on fatigue resistance of welded joints in steel orthotropic decks", *J. Bridge Eng.*, **14**(5), 366-373.
- Simo, J.C. and Taylor, R.L. (1985), "Consistent tangent operators for rate-independent elastoplasticity", *Comput. Method. Appl. Mech. Eng.*, **48**(1), 101-118.
- Xiao, Z.G., Yamada, K., Inoue, J. and Yamaguchi, K. (2006), "Fatigue cracks in longitudinal ribs of steel orthotropic deck", *Int. J. Fatigue*, **28**(4), 409-416.
- Xiao, Z., Yamada, K., Ya, S. and Zhao, X. (2008), "Stress analyses and fatigue evaluation of rib-to-deck joints in steel orthotropic decks", *Int. J. Fatigue*, **30**(8), 1387-1397.
- Ya, S., Yamada, K. and Ishikawa, T. (2011), "Fatigue evaluation of rib-to deck welded joints of orthotropic steel bridge deck", *J. Bridge Eng.*, **16**(4), 492-499.